Scaling Relations of Galaxy Clusters: X-ray and Lensing vs. Simulations

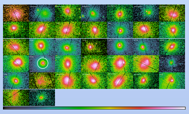

Yu-Ying Zhang[1,2], Alexis Finoguenov[2], Hans Böhringer[2], Jean-Paul Kneib[3], Graham P. Smith[4], Rüdiger Kneissl[5], Nobuhiro Okabe[6], Hakon Dahle[3], Thomas H. Reiprich[1]

[1]Argelander-Institut für Astronomie, Universität Bonn, Auf dem Hügel 71, 53121 Bonn, Germany
[2] Max-Planck-Institut für extraterrestrische Physik, Giessenbachstraße, 85748 Garching, Germany
[3] OAMP, Laboratoire d'Astrophysique de Marseille, traverse du Siphon, 13012 Marseille, France
[4] School of Physics and Astronomy, University of Birmingham, Edgbaston, Birmingham, B152TT, UK
[5] Max-Planck-Institut für Radioastronomie, Auf dem Hügel 69, 53121 Bonn, Germany
[6] Astronomical institute, Tohoku University, Aramaki, Aoba-ku, Sendai, 980-8578, Japan

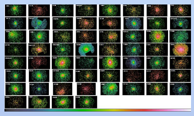

Abstract

Abstract: The Local Cluster Substructure Survey (LoCuSS, Smith et al.) is a systematic multi-wavelength survey of more than 100 X-ray luminous galaxy clusters in the redshift range 0.14-0.3 selected from the ROSAT All Sky Survey (RASS). We used data on 37 LoCuSS clusters from the *XMM-Newton* archive. The scaling relations based solely on the X-ray data obey empirical self-similarity. The mean of the X-ray based mass to weak lensing mass ratio of these clusters is ~ 1 with 31-51% scatter. The normalization of the M-Y_X relation using X-ray mass estimates is lower than the one from simulations by 18-24% at 3σ significance. This is in good agreement with the M-Y_X relation based on weak lensing masses, the normalization being $\sim 20\%$ lower than the one from simulations at 2σ significance. The average of the X-ray based mass to weak lensing mass ratio is 1.09 ± 0.08, setting the limit of the non-thermal pressure support to $9 \pm 8\%$. To better understand the systematics of cluster mass estimates, we attempt to use the *XMM-Newton* data of the HIghest X-ray FLUx Galaxy Cluster Sample (HIFLUGCS, Reiprich & Böhringer 02) to make a detailed comparison between radial profiles and 2-D maps. This will allow us to identify mergers and the departure from hydrostatic equilibrium. The LoCuSS sample at $z \sim 0.2$ and the HIFLUGCS sample at $z \sim 0$ complement each other and it is therefore a unique combination to serve the precision cluster cosmology.

LoCuSS vs. HIFLUGCS

Scientific Goals Robust cluster cosmology experiments require well calibrated measurements of the shape, scatter and evolution of the mass-observable scaling relations based on large statistical samples of clusters of galaxies that are unbiased with respect to cluster morphology. Elimination of systematic uncertainties from this calibration demands: (1) that the cluster mass measurements are cross-checked between independent mass measurement techniques, including X-ray and weak lensing approaches, and (2) that major cluster mergers and their effect on the systematics of cluster mass estimates are identified. *XMM-Newton*, with its large field-of-view (FOV), large effective area and high spectral resolution, for the first time allows us to compile large samples with good statistic to investigate the systematics of cluster mass estimates and to calibrate the mass-observable scaling relations.

LoCuSS vs. HIFLUGCS The main attractions of our approach are the well-defined sensitivity limit of such surveys and the minimal biases towards different cluster morphologies. The Local Cluster Substructure Survey (LoCuSS, PI: G. P. Smith) is such a systematic multi-wavelength survey of more than 100 galaxy clusters at $0.14 \lesssim z \lesssim 0.3$ selected from the RASS (Ebeling et al. 98, 00; Böhringer et al. 04). The HIghest X-ray FLUx Galaxy Cluster Sample (HIFLUGCS, PI: T.H. Reiprich) is also such a sample but nearby, consisting of 64 massive galaxy clusters selected from the RASS, of which 63 are observed by XMM-Newton. Both LoCuSS and HIFLUGCS provide morphology-unbiased samples of X-ray luminous galaxy clusters. The LoCuSS, at redshift bin of 0.2, better serves our first goal, and the HIFLUGCS, at redshift bin of 0.0, better serves the 2nd goal. The combination provides us a unique powerful tool for the precision cluster cosmology.

LoCuSS: X-ray and Lensing vs. Simulations (Zhang et al. 08)

Data

***XMM-Newton* observations** for 37 LoCuSS clusters in the archive have been analyzed to derive the X-ray observables and X-ray masses (Zhang et al. 08). With the large FOV of *XMM-Newton*, the X-ray mass profiles can be measured beyond r_{500}.

Weak lensing results for 19 clusters of the 37 LoCuSS clusters are published, 10 using large field data ($> r_{200}$, Bardeau et al. 07), and 15 using small field data ($\sim 0.4 r_{500}$, Dahle 06).

X-ray Results

Scaled profiles of the X-ray properties for the 37 LoCuSS clusters show structural-similarity beyond the cluster core ($> 0.2 r_{500}$). There is no pronounced cool core cluster and non-cool core cluster bi-modality.

X-ray scaling relations for the 37 LoCuSS clusters (S–T, S–Y_X, P–Y_X, M–T, M–Y_X, M–M_{gas}, M_{gas}–T, L–T, L–Y_X, and L–M) obey empirical self-similarity and reveal no additional evolution beyond the large-scale structure growth. For example, the M-Y_X relation of the 37 LoCuSS clusters agrees with the relations of the nearby samples in Arnaud et al. (07) and Kravtsov et al. (07) within 2%.

Scatter in the X-ray scaling relations is relatively low, e.g. 13% for M-Y_X. And the segregation between the sample of the 37 LoCuSS clusters and its subsample of non-cool core clusters is insignificant, e.g. within 5% for M-Y_X.

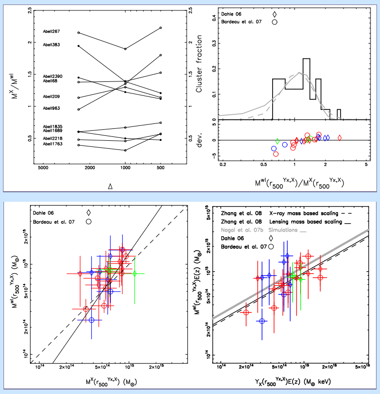

Figure 1: *Upper left:* X-ray to weak lensing mass ratio vs. overdensity. *Upper right:* Histogram of the weak lensing to X-ray mass ratio and its Gaussian fit. *Lower left:* Weak lensing mass vs. X-ray mass. *Lower right:* M-Y_X relation. $r_{500}^{Y_X,X}$ is defined by the mass profile at the ovedensity of 500, in which the mass profile is derived from the Y_X profile and the X-ray M-Y_X relation.

Lensing and X-ray vs. Simulations

Weak lensing to X-ray mass ratio shows (1) scatter almost independent on the chosen radius (*Upper left* in Figure 1, in prep.), (2) a mean value of ~ 1 using a Gaussian fit (*upper right* in Figure 1), indicating good agreement between X-ray and weak lensing masses for most clusters, (3) 31–51 per cent scatter derived from the Gaussian fit (*upper right* in Figure 1), and (4) an average of 1.09 ± 0.08 (*lower left* in Figure 1), indicating non-thermal pressure support within 9% at $r_{500}^{Y_X,X}$.

Mass - observable relations using X-ray masses and weak lensing masses, respectively, show a good agreement, e.g. within 6% for the M-Y_X relation (*lower right* in Figure 1). The scatter of the weak lensing mass based relations (e.g. 22% for M-Y_X) is higher than the scatter of the X-ray mass based relations (e.g. 13% for M-Y_X) by a factor of ~ 2.

Observed mass - observable relations using either X-ray masses or weak lensing masses are lower than the prediction from simulations by $\sim 20\%$, e.g. 24% for the X-ray mass based M-Y_X relation and 18% for the weak lensing mass based M-Y_X relation (*lower right* in Figure 1). The significance is $\sim 2\sigma$ for the weak lensing mass based relations and $\sim 3\sigma$ for the X-ray mass based relations.

HIFLUGCS: Profile vs. 2-D map (Zhang et al. in prep.)

Data and Reduction Strategy

63 HIFLUGCS clusters have been observed by *XMM-Newton* (148 pointings) with ~ 2.2 Ms (~ 1.8 Ms) clean exposure time for MOS (pn).

Background subtraction method follows the philosophy in Snowden et al. (08) with some complications adjusted to our project. For example, we used ROSAT PSPC pointed observations to assist the modeling of the CXB and we extended the reduction also to the pn data.

Width of annuli for spectral analysis are determined by (1) that the width of each annulus is $\geq 0.5'$, (2) that the signal-to-noise ratio is greater than C per MOS2 spectrum in the 0.5-7.8 keV band. The threshold C is 135 except for the clusters with less than 4 annuli in total for which C is 75.

2-D Mask for the map analysis is determined by the weighted Voronoi tesselation method (Cappellari & Copin 03, Diehl & Statler 06) to bin the MOS2 $4'' \times 4''$ binned image in the 0.5-2.0 keV band to a signal-to-noise ratio of > 33. The spectral analysis is performed in each regional bin to determine the temperature, abundance and their errors to create the temperature and abundace maps and their error maps.

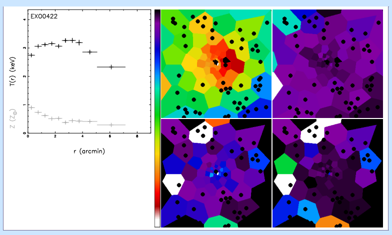

Figure 2: *Left:* Temperature (black) and metallicity (grey) profiles. *Right:* Temperature map and its error map in units of keV on top and metallicity map and its error map in units of solar metallicity on bottom. The map box is $\sim 22' \times 22'$ with the north towards the right and the east towards the top. The scale bar is in linear scale ranging from 0.0 to 4.2. The filled black circles in the maps are the regions for the point sources, which are subtracted prior to the spectral and map analysis.

One Example: EXO 0422

Temperature and metallicity profiles for EXO 0422 (*left* in Figure 2). The profiles serve as the reference curves for the cluster.

Temperature and metallicity maps for EXO 0422 (*right* in Figure 2). Despite the regular appearance of the temperature/abundance profile and also the surface brightness map, the temperature/abundance map reveals some small but significant fluctuations from the profile. The fluctuations and indicated cold fronts and shocks in temperature, entropy and pressure maps will be used to investigate the cluster dynamics.

HIFLUGCS Short Term Goal

Profile vs. 2-D map comparison in a statistical way for the HIFLUGCS provides a global view for a representative sample of massive galaxy clusters on: (1) merging fractions indicated by different merging features, (2) effects of merging on the mass systematics caused by deviations from hydrostatic equilibrium, and (3) the scatter in the scaling relations introduced by merging clusters. Such studies complement the LoCuSS by providing the knowledge to constrain the physics behind the X-ray scaling relations and their scatter.

References

Reiprich, T.H. & Böhringer, H. 2002, ApJ, 567, 716
Zhang, Y.-Y., Finoguenov, A., Böhringer, H., Kneib, J.-P., Smith, G. P., Kneissl, R., Okabe, N., & Dahle, H. 2008, A&A, 482, 451

Acknowledgments

YYZ acknlowdges G.W. Pratt, A. Vikhlinin, T.J. Ponman, A.E. Evrard, A. Babul, P. Mazzotta, G. Hasinger, D. Pierini, A. Mahdavi, and D. Hudson for their kind suggestions and useful discussions.

Contact: yyzhang@astro.uni-bonn.de